

# Gluon propagator and zero-momentum modes on the lattice \*

G. Damm <sup>a</sup>, W. Kerler <sup>a,b</sup>, V.K. Mitrjushkin <sup>c</sup>

<sup>a</sup>Fachbereich Physik, Universität Marburg, D-35032 Marburg, Germany

<sup>b</sup>Institut für Physik, Humboldt-Universität, D-10115 Berlin, Germany

<sup>c</sup>Joint Institute for Nuclear Research, Dubna, Russia

We investigate the propagators of 4D SU(2) gauge theory in Landau gauge by Monte Carlo simulations. To be able to compare with perturbative calculations we use large  $\beta$  values. There the breaking of the Z(2) symmetry causes large effects for all four lattice directions and doing the analysis in the appropriate state gets important. We find that the gluon propagator in the weak-coupling limit is strongly affected by zero-momentum modes.

## 1. INTRODUCTION

Starting with Ref. [1] there has been a number of nonperturbative lattice studies of the gluon propagator in Landau gauge. However, the impact of zero-momentum modes on the propagators has not been analyzed. Recently one of us has shown that zero-momentum modes may strongly affect gauge-dependent correlators [2]. Therefore, we have performed simulations in 4D SU2 lattice gauge theory to clarify this issue.

To be able to compare quantitatively with perturbative calculations large  $\beta$  values must be used. There the propagators, which gauge fixing effectively makes very nonlocal objects, become sensitive to the broken Z(2) symmetry states of the deconfinement region. For comparison with perturbative results the appropriate one of these states has to be selected.

We use the Wilson action, periodic boundary conditions, fields  $\mathcal{O}_\mu(x) = \frac{1}{2i}(U_{\mu x} - U_{\mu x}^\dagger)$  and the Landau gauge. The propagators considered are

$$\Gamma_\mu(\vec{p}, \tau) = \frac{1}{L_4} \sum_t \text{Tr} \langle \tilde{\mathcal{O}}_\mu(\vec{p}, t + \tau) \tilde{\mathcal{O}}_\mu(-\vec{p}, t) \rangle \quad (1.1)$$

where  $\tilde{\mathcal{O}}_\mu(\vec{p}, \tau) = \frac{1}{V_3} \sum_{\vec{x}} e^{i\vec{p} \cdot \vec{x}} \mathcal{O}(\vec{x}, \tau)$ . Choosing  $\vec{p} = (0, 0, p_3)$  where  $p_3 = \frac{2\pi}{L_3} \rho$  the transverse propagator is defined by  $\Gamma_T = \frac{1}{2}(\Gamma_1 + \Gamma_2)$ .

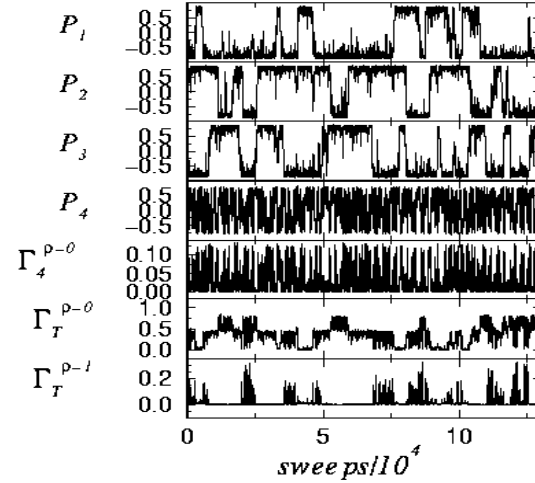


Figure 1. Time history of Polyakov loops and ( $\tau = 0$ ) propagators at  $\beta = 10$  on  $4^3 \times 8$  lattice.

## 2. BROKEN Z(2) SYMMETRY

In our simulations on lattices of sizes  $4^3 \times 8$ ,  $8^3 \times 16$  and  $16^3 \times 32$  we have used Polyakov loops  $P_\mu = \frac{L_\mu}{V_4} \sum_{x \neq x_\mu} \text{Tr} \prod_{x_\mu} U_{\mu x}$  to monitor the breaking of the Z(2) symmetry. According to the two possibilities for each direction (i.e.,  $P_\mu > 0$  or  $P_\mu < 0$ ) there are 16 states:  $(++++)$ ,  $(+++-)$ ,  $\dots$ ,  $(----)$ .

The time histories of the  $P_\mu$ ,  $\Gamma_T$  and  $\Gamma_4$  in Fig. 1 illustrate that the  $\Gamma_\mu$  are, in fact, strongly affected by the indicated states. This phenomenon has been observed on all lattices consid-

\*Contribution to Lattice '97, International Symposium, Edinburgh, UK, 1997. This research was supported in part under DFG grants Ke 250/13-1 and Mu 932/1-4.

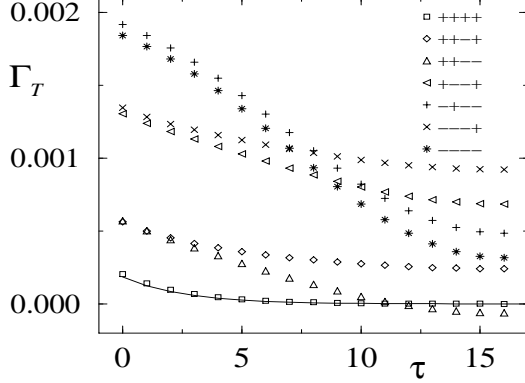


Figure 2.  $\Gamma_T(\vec{p}, \tau)$  in various states for  $\rho = 1$ ,  $\beta = 10$  and  $16^3 \times 32$  lattice (solid line is (3.1)).

ered. From the numerical analysis we find in more detail that the observables take different values in different states. As one can see in Fig. 2, (+++++) gives results consistent with perturbation theory while otherwise large deviations occur.

### 3. FORMS OF PROPAGATORS

In the limit of large  $\beta = 4/g^2$  one obtains in lowest-order approximation

$$\Gamma_T(\vec{p}, \tau) \rightarrow \frac{3g^2}{2V_4} \sum_{p_4} \frac{e^{-ip_4\tau}}{4\sin^2 \frac{p_3}{2} + 4\sin^2 \frac{p_4}{2}} \quad (3.1)$$

provided that  $p_3 \neq 0$ . To handle  $\vec{p} = 0$  we split off the zero-four-momentum part  $C_\mu = \frac{1}{V_4} \sum_x \mathcal{O}_\mu(x)$  so that the fields decompose as  $\tilde{\mathcal{O}}_\mu(\vec{0}, \tau) = C_\mu + \delta\tilde{\mathcal{O}}_\mu(\tau)$  and (1.1) becomes

$$\Gamma_\mu(\vec{0}, \tau) = \text{Tr}\langle C_\mu^2 \rangle + R_\mu(\tau); \quad (3.2)$$

$$R_\mu(\tau) = \frac{1}{L_4} \sum_t \text{Tr}\langle \delta\tilde{\mathcal{O}}_\mu(t+\tau) \delta\tilde{\mathcal{O}}_\mu(t) \rangle \quad (3.3)$$

The evaluation of (3.3) by collective-coordinate methods only works in the lowest-order approximation and leads to

$$\Gamma_\mu(\vec{0}, \tau) \rightarrow \text{Tr}\langle C_\mu^2 \rangle + \frac{3g^2}{2V_4} \sum_{p_4 \neq 0} \frac{e^{-ip_4\tau}}{4\sin^2 \frac{p_4}{2}}. \quad (3.4)$$

### 4. ZERO-MOMENTUM MODES

Now we restrict the considerations to data of the (++++)-state. First we note important

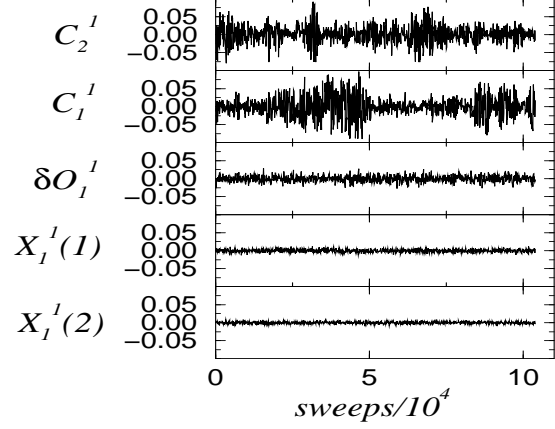


Figure 3. Time histories of  $C_\mu^a$ ,  $\delta\tilde{\mathcal{O}}_\mu^a$ ,  $X_\mu^a(1)$  and  $X_\mu^a(2)$  for  $\beta = 10$  and  $16^3 \times 32$  lattice.

properties of  $C_\mu$  by comparing the time histories of  $C_\mu$ ,  $\delta\tilde{\mathcal{O}}_\mu(\tau)$  and  $X_\mu(\rho) = \text{Re} \frac{1}{V_4} \sum_x e^{i\vec{p}\cdot\vec{x}} \mathcal{O}_\mu(x)$  with  $\vec{p} = (0, 0, \frac{2\pi}{L_3}\rho)$  and  $\rho \neq 0$ , i.e. of an example of a nonzero-momentum part of the fields. Fig. 3 shows behaviors of components  $C_\mu^a$ ,  $\delta\tilde{\mathcal{O}}_\mu^a$  and  $X_\mu^a$  (where  $C_\mu = \sum_a (\sigma^a/2) C_\mu^a$  etc.). For  $\delta\tilde{\mathcal{O}}_\mu^a$ ,  $X_\mu^a(1)$  and  $X_\mu^a(2)$  uniform Monte Carlo noise is seen. Its magnitude is larger if the three-momentum involved in the particular quantity gets smaller. For  $C_\mu^a$  in addition to such noise, with magnitude comparable to that of  $\delta\tilde{\mathcal{O}}_\mu^a$ , surprisingly large variations are observed. These variations exhibit different patterns for different  $\mu$ , while for different  $a$  we find essentially the same pattern.

In the decomposition of the fields  $\tilde{\mathcal{O}}_\mu$  the parts  $C_\mu$  and  $\delta\tilde{\mathcal{O}}_\mu$  obviously behave quite differently. The observed large variations of  $C_\mu^a$  appear to be a characteristic consequence of zero-momentum modes.

In addition to  $\Gamma_T(\vec{0}, \tau)$  and  $R_T(\tau)$  also the quantity  $\text{Tr}\langle C_T^2 \rangle$  needed for the comparison with (3.4) has been determined in the simulations. From Fig. 4 it is obvious that our numerical results for the transverse propagator with  $\vec{p} = \vec{0}$  agree reasonably well with that of our lowest-order calculation (3.4). It is seen that the zero-momentum part  $\text{Tr}\langle C_T^2 \rangle$  is large as compared to the rest, which is related to the large variations of  $C_\mu$  mentioned above. It is also apparent that while  $\Gamma_T(\vec{0}, \tau)$  exhibits unusually large errors, which stem from the large variations of  $C_\mu$ ,

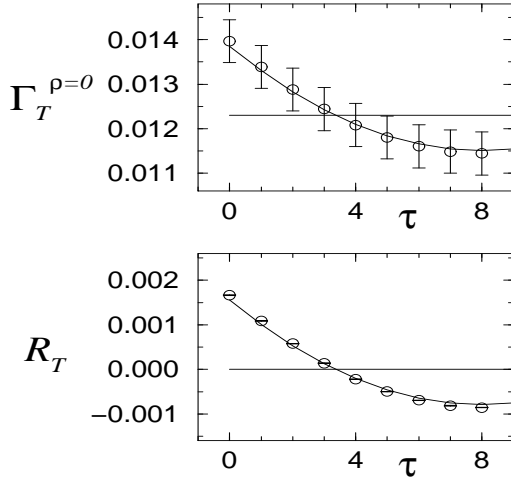


Figure 4.  $\Gamma_T(\vec{0}, \tau)$  and  $R_T(\tau)$  compared with (3.4) (curves) and  $\text{Tr}\langle C_\mu^2 \rangle$  (constant line in upper Figure) for  $\beta = 10$  and  $8^3 \times 16$  lattice.

for  $R_T(\tau)$  one gets errors of usual size. Analogous observations as for the  $8^3 \times 16$  lattice with  $\beta = 10$  have been made on  $4^3 \times 8$  with  $\beta = 10$  and on  $16^3 \times 32$  with  $\beta = 10$  and  $\beta = 99$ . Thus our numerical results confirm the description we have given.

The importance of zero-momentum modes is quantified by the fact that  $\text{Tr}\langle C_\mu^2 \rangle$  is large as compared to  $R_\mu(0)$ . To compare different lattice sizes and different values of  $\beta$  the respective values are to be multiplied by  $V_3/g^2$  (which obviously cancels the extra factor implicit in our definitions). It turns out that the values of  $\zeta = (V_3/g^2)\text{Tr}\langle C_T^2 \rangle$  are much larger than  $\gamma = (V_3/g^2)(R_T(0) - R_T(L_4/2))$ . From Table 1 it is seen that for increasing  $\beta$  this feature gets even more pronounced. The same holds for increasing lattice size. Not only  $\zeta$  gets larger but there is also an increase of the ratios  $\zeta/\gamma$ .

Table 1

lattice	$\beta$	$\zeta$	$\gamma$
$4^3 \times 8$	10	6.30 (16)	1.610 (5)
$8^3 \times 16$	10	15.7 (7)	3.229 (17)
$16^3 \times 32$	10	57 (10)	6.03 (22)
$16^3 \times 32$	99	375 (86)	4.98 (19)

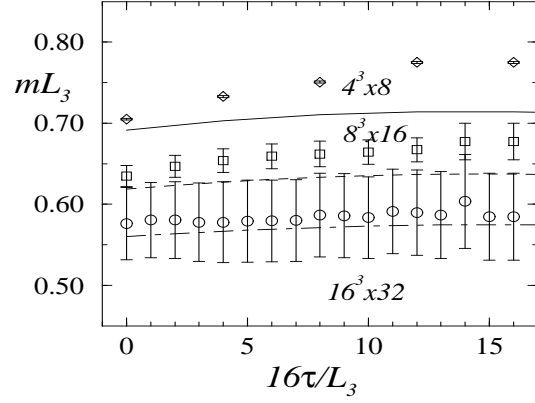


Figure 5. Misleading results from determinations of effective masses from eq. (4.1) for  $\vec{p} = \vec{0}$ ,  $\beta = 10$ . Curves are based on eq. (3.4).

To show that the usual determination of effective masses  $m(\tau)$  can be misleading if zero-momentum modes are present we have also calculated  $m(\tau)$  from

$$\frac{\cosh(m(\tau)(\tau + 1 - \frac{L_4}{2}))}{\cosh(m(\tau)(\tau - \frac{L_4}{2}))} = \frac{\Gamma_T(\vec{0}, \tau + 1)}{\Gamma_T(\vec{0}, \tau)}. \quad (4.1)$$

From Fig. 5 it is seen that even at very weak coupling, where the situation clearly is described by (3.4), a gluon mass is imitated. Its decrease with lattice size actually reflects the increase of the zero-momentum contribution. Because  $m(\tau)L_\mu$  shows little dependence on lattice size, the present results may also be considered from the point of view of finite temperatures where screening masses are determined [3].

To summarize, at  $\beta$ -values considered here such masses are fake. The question of the role of the zero-momentum modes at smaller values of  $\beta$  (in the physical region) needs further study.

One of us (W.K.) wishes to thank M. Müller-Preussker and his group for their kind hospitality.

## REFERENCES

1. J.E. Mandula and M. Ogilvie, Phys. Lett. B 185 (1987) 127.
2. V.K. Mitrjushkin, Phys. Lett. B 390 (1997) 293.
3. U.M. Heller, F. Karsch and J. Rank, Phys. Lett. B 355 (1995) 511.